

Designing Turbine Blades for Fatigue and Creep

Bruno Dambrine and Jean Pierre Mascarell

*Société Nationale D'Étude Et De Construction De Moteurs D'Aviation (SNECMA)
2, Boulevard Victor, 75724 Paris Cedex 15*

1. INTRODUCTION

Steady progress in the performance of turbojets for civilian and military aircraft propulsion involves increasing the Turbine Entry Temperature (TET). So it is not astonishing to observe, as Fig. 1 shows, that TET has been increasing at a rate of some 15°C per year over the last twenty years; and it is generally felt that this trend will continue.

The materials as such have certainly not been the only factors at play in raising the TET, as their creep strength has improved at the slower annual rate of 5 to 7°C during the same period. Rather, an essential part of the advance in TET comes from the application of new blade cooling techniques at SNECMA, along with improvements in blade life prediction methods.

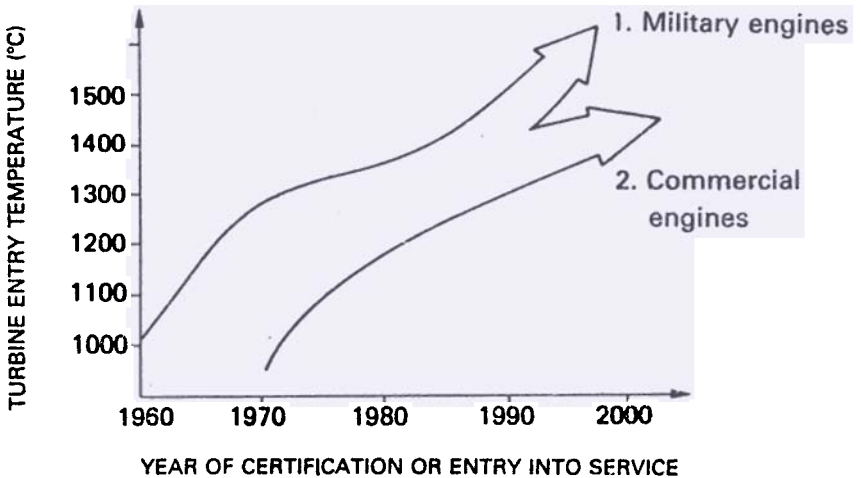


Figure 1. Trend in turbine intake temperatures.

Figures 2 and 3 illustrate^{1,2} the evolution of cooling techniques. Due to the effectiveness of these cooling techniques, intense thermal gradients are generated during speed transients; so any mechanical analysis requires a prior thermal analysis.

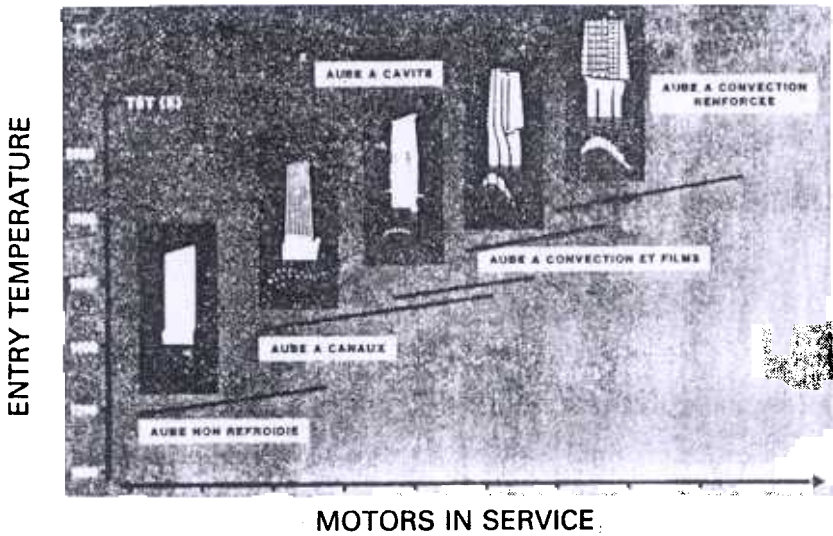


Figure 2. 1. Blade with cavity, 2. Blade with boosted convection, 3. Blade with convection and films, 4. Blade with channels, 5. Uncooled blade.

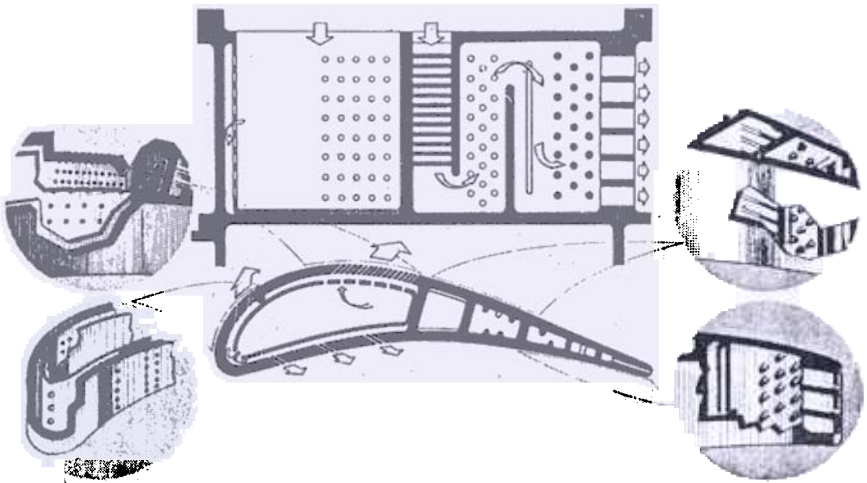


Figure 3. Various cooling techniques.

2. TEMPERATURE FIELD COMPUTATIONS

The temperature fields are established for both transient and stabilized conditions and, as explained² in ref. 2 are the result of a set of studies on :

- the transfer coefficient distribution over the external walls of the blade, by computing the heat flux transfer between the boundary layer and the walls;

- the effectiveness of the films and their interaction with the boundary layer, to optimize the position of the emission areas and the distribution, density, diameter and inclination of the holes;
- the effectiveness of internal convection cooling and various means of improving the transfer coefficients (impact cooling, flow disturbance generators, bridges, barbs);
- the temperature fields in the various cross sections of the blade in steady rating, computed by two- and three-dimensional finite element methods, and also at various points in a transient rating.

Figure 4 shows a computed temperature distribution through the median section of a cooled blade, compared with optical pyrometer data. The impact such temperature gradients have on the mechanical properties is particularly harmful during the transient phases³ (Fig. 5 ref. 3): those parts subject to high heat transfer coefficients, such as the leading edge, heat up and cool off much faster than the parts inside that are exposed only to the cooling flows.

So during the transient phases, temperature gradient inversions appear that increase the amplitude of the mechanical stresses.

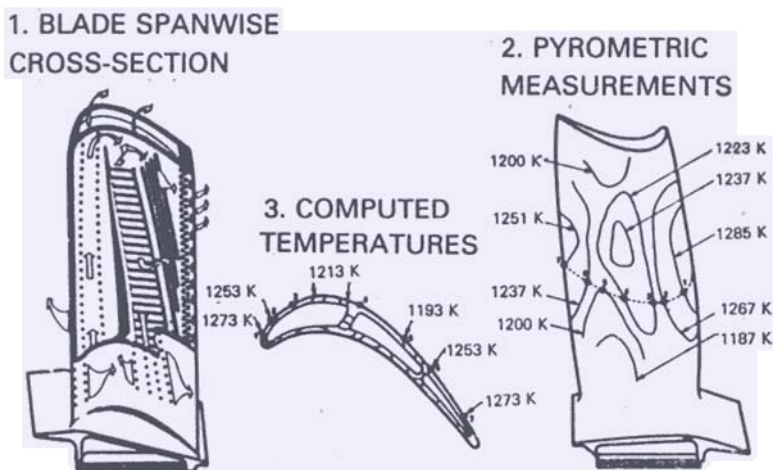


Figure 4. Skin temperatures of a film and convection-cooled blade.

3. LIFE PREDICTION

The case of cooled blades where fatigue and creep damage accumulate will be discussed here. This is a case for which we have, in collaboration with ONERA, created a new method of life prediction.

When we analyse a blade temperature field (Fig. 4), we observe that the isotherms are almost radial, which leads to the conclusion that the thermal stresses generated by multi-directional heat expansion vectors are also radial and, consequently, in the same direction as the centrifugal stresses. A blade section can thus be modeled by a set of axial finite elements comparable to tension-compression loaded bars. By adding

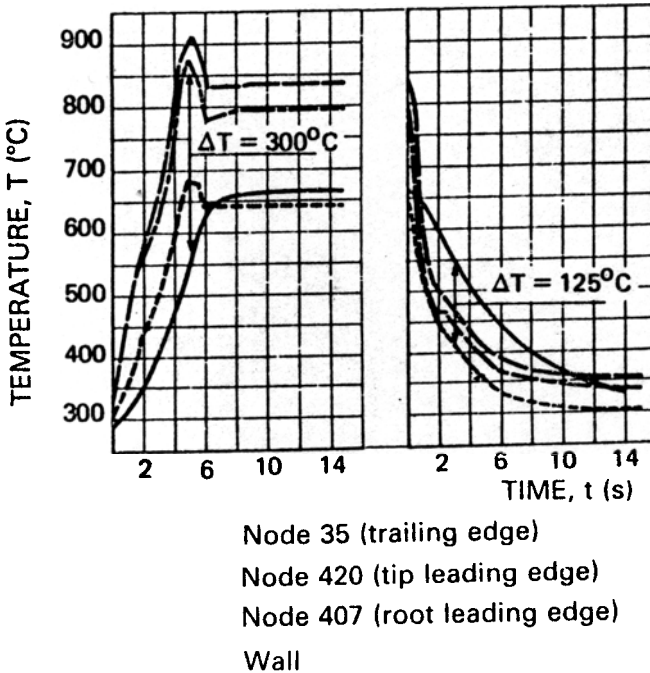


Figure 5. Transient variation of the temperatures.

hypotheses concerning the deformation of the section (radial displacement and cross section rotations) and the associated forces (radial stress and bending moments), we get a perfectly defined system provided the material behaviour, i.e., the strain-stress relationship, is known, such relationship being temperature-dependent.

The advantage of the monoaxial model has also been demonstrated⁴ by NASA-Lewis and SNECMA where the radial and equivalent stresses are compared by way of a three-dimensional viscoplastic simulation of a turbine blade.

The CALIFAT blade life prediction program developed by ONERA⁵ uses this approach to determine the time variations of the stress and strain for all elements of the model, from which we can then predict :

- the creep damage resulting from high temperature stressing, at high levels of stress and depending on the length of time these conditions are held;
- fatigue damage resulting from successive variations in the amplitude of centrifugal and thermal stresses during operating cycles.

This data can be used to predict the critical point of the blade and the failure mode, and this may lead to modifications in the cooling arrangement to minimize the thermal stresses and increase the life of the component.

We will now look in detail into :

the constitutive equations of the material, to model the viscoplastic effects under cyclic loading⁶;

the structure of a finite element program used to simulate cyclic viscoplastic behaviour⁷;

the continuum damage method, to predict life⁸

4. BEHAVIOUR OF THE MATERIAL

To predict the life of components, or more precisely the time to crack initiation, the constitutive equations of the materials must be known, i.e. the stress-strain relationships as a function of time, of temperature and of hardening, in order to be able to compute the stresses and strains in the component. We will not go into, here, the formulas developed and used at ONERA, but let us simply say that these viscoplasticity laws are based on the principle of the local state and the concept of internal variables to describe the current state of the volume element.

The various laws used are :

- (i) The Norton law, which adequately describes the secondary creep part, is written in the form

$$\dot{\varepsilon}_p^o = \left(\frac{\sigma}{K} \right)^n$$

The coefficients are identified by means of creep tests at several levels of stress.

- (ii) The Lemaitre law, which describes the increasing monotonic viscoplastic phenomena and correctly models the tensile, creep (primary and secondary), and relaxation tests, and is expressed in the form.

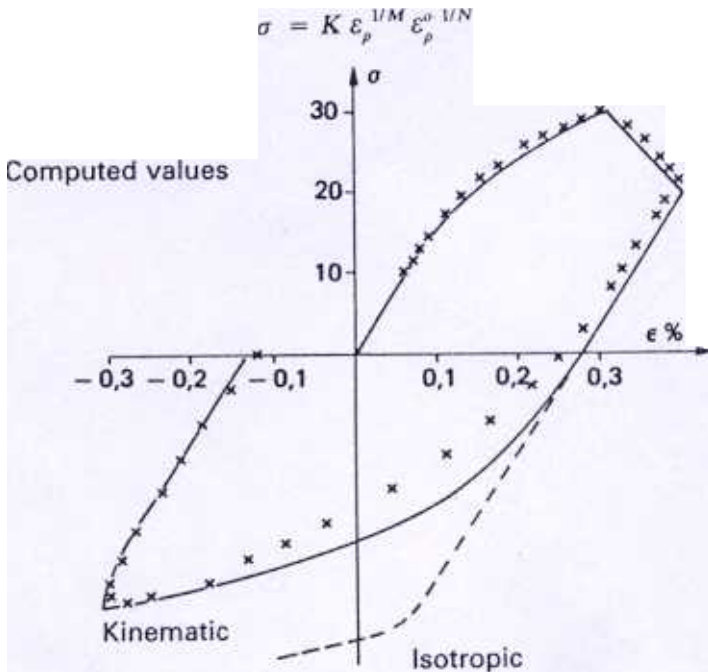


Figure 6. Stress-elongation relations for monodimensional tensile compressive loading.

The three temperature-dependant coefficients are identified from creep, relaxation and tensile testing. The use of this law is to describe cyclic loadings entails, for example, an isotropic work hardening hypothesis which, cannot describe the Bauschinger effect satisfactorily as shown in Fig. 6.

(iii) The five-parameter law, breaks the stress down into three terms (Fig. 7)

$$\text{Viscous stress } \sigma_v = K \epsilon_p^{1/N}$$

Isotropic stress R describes the size of the elastic area in the stabilized cycle:

Nonlinear kinematic stress $X = C (a \epsilon_p^o - X |\epsilon_p|)$ which describes the translation of the elastic domain during cycling.

The law is written in the form

$$\epsilon_p^o = \frac{\langle |\sigma - X| - R \rangle^N \text{sign}(\sigma - X)}{K}$$

in which

$$\langle v \rangle = v \quad \text{if } v \geq 0, \quad \langle v \rangle = 0 \quad \text{if } v < 0.$$

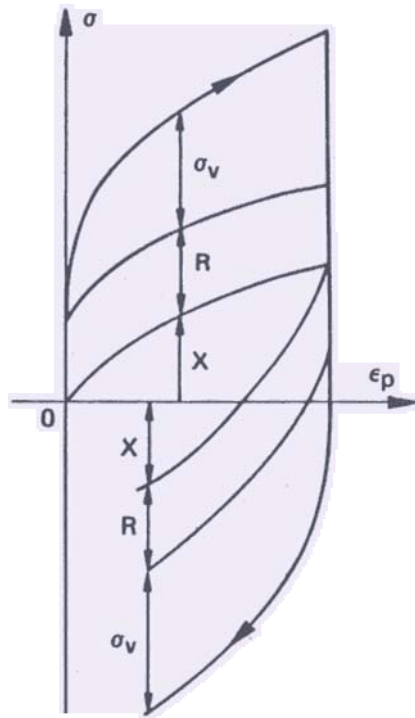


Figure 7.

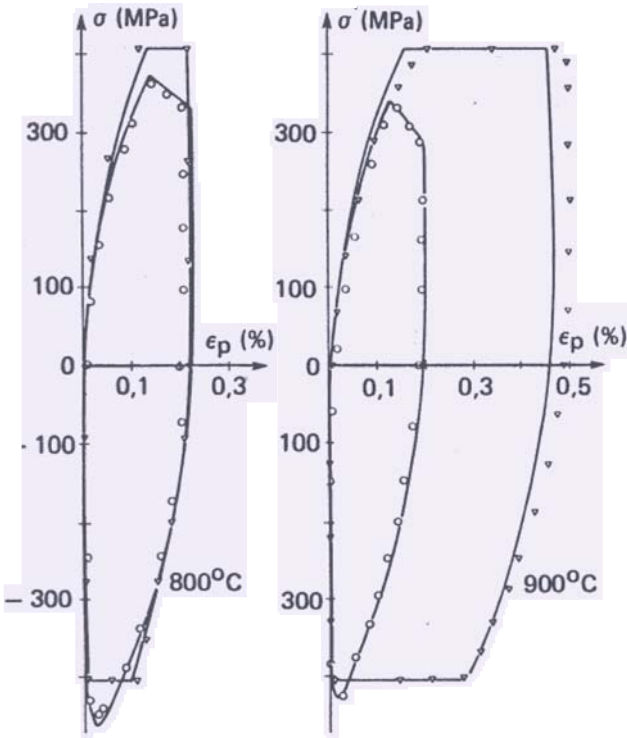


Figure 8.

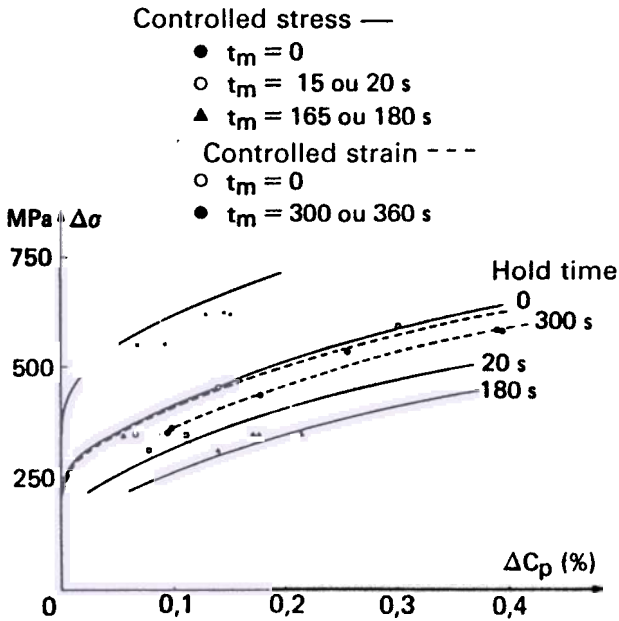


Figure 9.

This law provides a good model of the stabilized cyclic behaviour of the material, as Figs. 8 and 9 shows for the IN 100 alloy. In a strain domain limited to 0.5 per cent, the model adequately reproduces the cyclic curves, the hysteresis loops and the effect of the loading rate and hold time in the cyclic creep tests.

The constitutive equation does not describe the microstructural changes of the material that may occur at high temperature levels to which the material may be submitted for short periods.

The material is characterized at constant temperature, so for each temperature the coefficients affecting the law have to be determined by running a sufficient number of different tests to eliminate any undetermined values. In Fig. 10, the variations of the 5 parameter law coefficients are plotted against the temperature for the IN 100. These coefficients have been identified at SNECMA for MARM 509, DS 200 HF and Rene 77.

The coefficients are determined for several temperature levels; but as section 2 demonstrates, the computations must be made for a varying temperature. The models used were developed and identified for isothermal computations, but can reveal the temperature history effect as shown in Fig. 11 comparing a stress-strain loop as measured in anisothermal fatigue tests on IN 100 with the simulation made by the cyclic viscoplasticity module of the SAMCEF finite element code. The computed loop is stabilized after about two computation cycling. This example of mechanical stress-strain hysteresis loop for a thermal cycling between 600 and 1,050°C, with phase

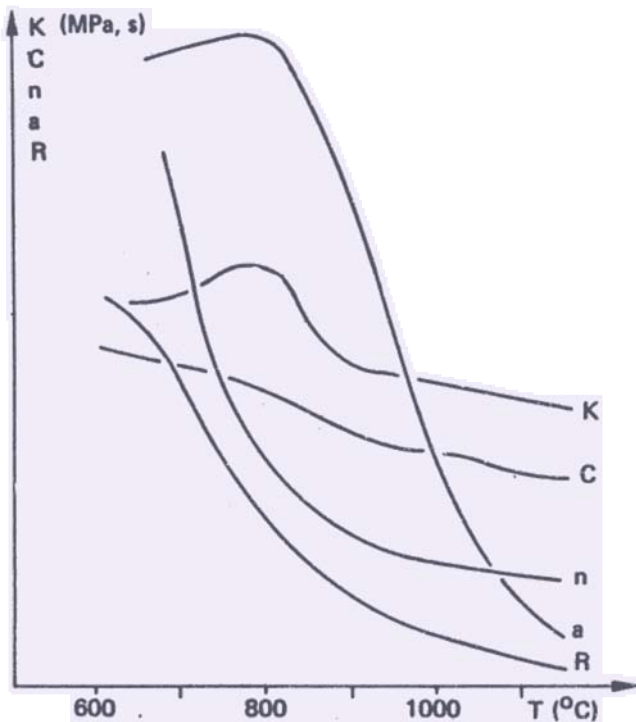


Figure 10.

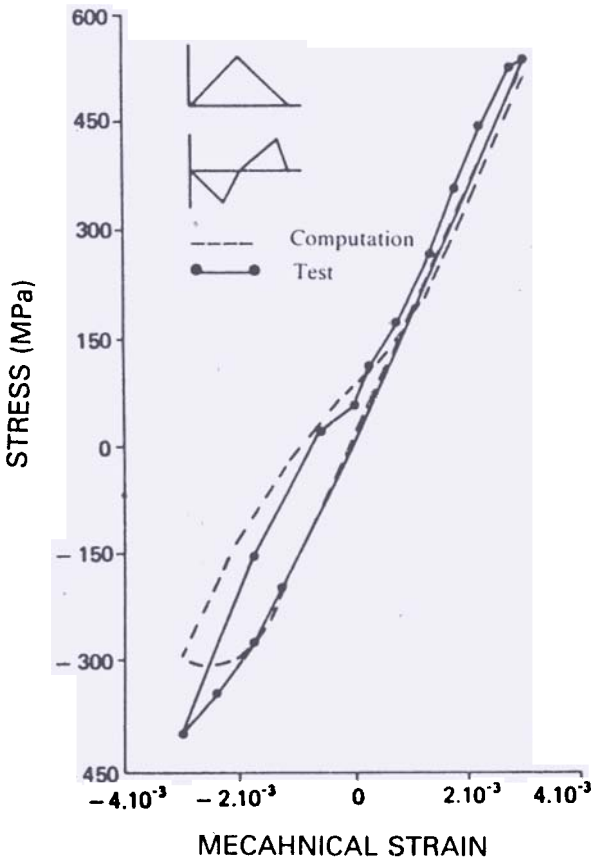


Figure 11.

shifted strain and temperature, shows the validity of the five-parameter law used to model these phenomena.

The shape of these loops depends strongly on the material used, whether it is an alloy that creeps a great deal like MARM 509, or relatively little like IN 100; and the anisothermal fatigue tests can generate a very large experimental database for validating these models and coefficients specific to the material⁹.

5. STRUCTURE OF A VISCOPLASTIC CODE

Calculating the response of a viscoplastic component raises the problem of solving the equations of equilibrium, if we use the finite element method, as well as the problem of time integration of the viscoplastic strain and work hardening variables.

The total strain, which we separate into elastic, viscoplastic and thermal, is written

$$\epsilon = \epsilon^e + \epsilon^{vp} + \epsilon^{\theta}$$

With the viscoplastic part governed by the previous laws, which makes it possible to write the equation of equilibrium in the form

$$[K] [q]^s = [F] + [f^{vp}] + [f^{\theta}]$$

in which the external, viscoplastic and thermal forces are all grouped together on the right: The viscoplastic forces are a function of the viscoplastic strain.

So the computation procedure is very simple, i.e. solve the equilibrium equation, compute the viscoplastic strain, compute the optimum step, and compute values for the following instant in time.

$$\begin{aligned}\sigma &= \text{LOCAL STRESS} \\ \sigma_a &= \text{AVERAGE CENTRIFUGAL STRESS} \\ &\quad \text{AT MAX SPEED}\end{aligned}$$

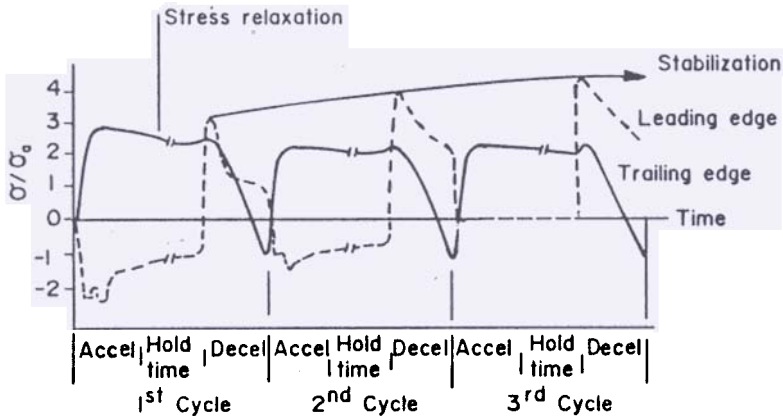


Figure 12. Computed stress variation in a cooled blade,

This method avoids computing a stiffness matrix at each increment. The non-linear effects are introduced in the second member. The CALIFAT code is an explicit Euler type code dedicated to blade computation with optimum step computation.

Fig. 12 shows how the stress state stabilizes, considering the material, the type of loading and the stress redistribution. This shows that to obtain a fair idea of the state, several cycles have to be computed until convergence this state is achieved each cycle being broken down into enough steps to follow the loading history closely.

6. DAMAGE COMPUTATION

The approach proposed⁸ for a volume element tells us that a material is free from damage if, free from microscopic crack or cavity, the final stage corresponding to failure due to a macroscopic crack. The damage phenomena are :

(i) the viscoplastic damage or creep due to the hold time at high temperature and stress level, (ii) the fatigue damage due to repeated stress cycles.

It can be seen that, once the history of the stress, strain and temperature is known, the damage laws can be used to determine the time or number of cycles leading to crack initiation. These laws are written using a damage variable D varying from 0 to 1.

The creep damage law used for designing the blades is that of Kachanov, along with another coefficient proposed by Rabotnov. This law applies very well to tensile damage, and few studies have been made on compressive damage.

The pure fatigue life is predicted using a criterion that is a function of the mean and maximum stress levels during the cycle. There is a particular problem in expressing the effect of a varying temperature. This is solved by defining an equivalent temperature, i.e. one giving the same damage for an isothermal cycle. The computed stress is normalized with respect to the temperature-dependent tensile failure stress $\sigma_{\text{failure}}(T)$ and the temperature corresponding to the maximum ratio $\sigma_{\text{failure}}(T)$ is used.

At high temperature, the two processes due to the loading cycles and loading time may interact. For this, the effects of fatigue and creep damage are assumed to be additive and the damage variable used in the two laws is taken as $dD = dD_c + dD_f$.

Figure 13 compares all of the data for the stress- and strain-controlled fatigue and for pure creep tests, for fatigue tests at two levels of temperature and stress, tests of creep after fatigue, and the differences are within a factor less than two, which is a good verification of the model.

In this type of model, the effect of the environment is ignored. Yet it is observed that the thermal fatigue cracks initiate at the carbides and at the oxidized grain boundaries. Other models are proposed where the time effect is not assimilated to creep but to oxidation⁹.

This damage model can account directly for the effect of oxidation and the oxygen embrittlement at crack tip. It has yielded very encouraging results for life predictions of thermal fatigue wedge specimens in MARM 509 and compact tension specimens in IN 100.

- * The internal damage variable D characterises the strength of the damaged material, including the microscopic damage introduced by the cyclic loading.
- * $D=0$ in the initial undamaged state, $D=1$ at specimen failure.
- * Creep damage

$$dD_c = \left(\frac{\sigma}{A} \right)^r (1-D)^{-k} dt$$

- * Fatigue damage

$$dD_f = \left[1 - (1-D)^{\beta+1} \right]^{\alpha(\sigma_M, \bar{\sigma}_M)} \times \left[\frac{\sigma_M - \bar{\sigma}}{M(\bar{\sigma})(1-D)} \right]^{\beta} dN$$

- * Fatigue-creep interaction

$$dD = dD_c + dD_f$$

- * r, k, A and β are temperature dependent coefficients and α and M are functions.

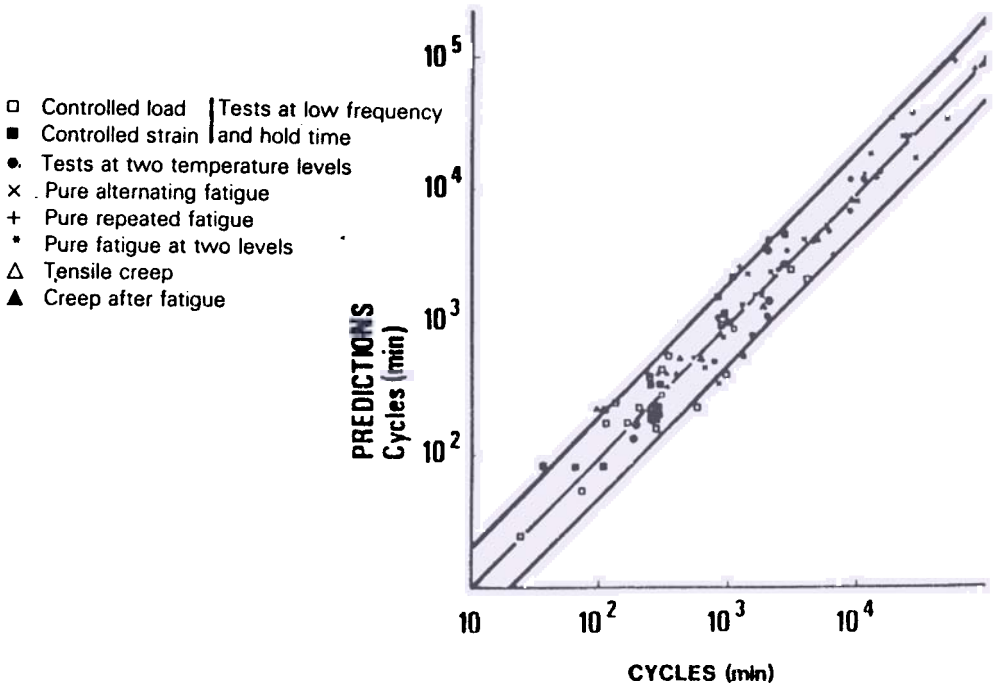


Figure 13. Life prediction by the continuum damage approach.

Fig. 14 reviews all of the method discussed. Efforts have yet to be made in three-dimensional viscoplastic computations, modelling of creep under compression – quite common in blades – and also modelling new materials such as single crystal alloys which will be one of the solutions to be applied to blades operating at high temperature.

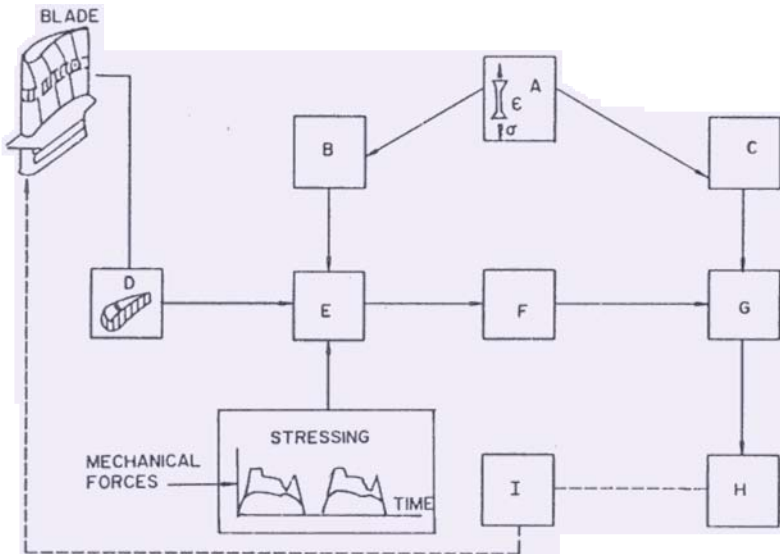


Figure 14.

Key to Fig. 14.

- A Isothermal tests – creep, relaxation, fatigue – on test specimens
- B Cyclic elastoviscoplastic constitutive equations
 $\sigma = f(\epsilon_a, \epsilon_p)$; $\dot{\epsilon}_p = g(\sigma, \epsilon_p)$
- C Failure laws in pure fatigue, pure creep and fatigue creep
- D Schematic representation
- E Computation program
- F For any element of the model $\sigma = f(t)$; $\epsilon = f(t)$ for successive cycles
- G For any element of the model computation of life to failure
- H Determination of the critical point and life of the airfoil
Blade redefinition

7. EXPERIMENTAL VALIDATION

The comparison of data measured on monoaxial tests specimens with model-generated data shows that the computed data are very close to reality. However, the transposition to actual components raises a few problems concerning the validity of the simplifications already made (space or time discretization, accuracy of the laws, material properties, etc...) and for this, we currently conduct tests of cooled turbine blades on a thermal fatigue test rig. These tests are run in an environment close to engine running conditions, and sufficiently well known to avoid any major cumulative uncertainties or approximations.

The factors not included in the CALIFAT program that might affect the predictions are essentially the thermal field and the forces applied. This is why the tests are carried out with constant gas temperature and blade loading while cycling the temperature by varying the cooling airflow in the blade.

Fig. 15 shows the test setup. The initial test program showed good reproducibility of the thermal conditions, which opens the door to blade endurance tests by way of superimposing thermal and mechanical stresses. One problem with this setup is how to apply a mechanical force equivalent to the centrifugal forces, as required to obtain a mean stress in the tested blade close to the level applied under engine conditions. The solution adopted was to apply a bending force along the major axis of inertia of the airfoil to simulate the mechanical loading in the leading and trailing edge areas. This is consistent with observations made on the engine, since these two areas are the most critical in rotor blades.

The result of a thermal cycling test on a blade made of IN 100 is shown in Fig. 16.

The initial data currently being analyzed shows a discrepancy by a factor of two between the predicted and experimental findings.

8. SINGLE CRYSTAL ALLOYS, THE KEY TO HIGH TEMPERATURES

From the original iron-nickel alloys up to the most recent single crystal materials, the increase by more than ten in the allowable creep failure stress in 10,000 hours,

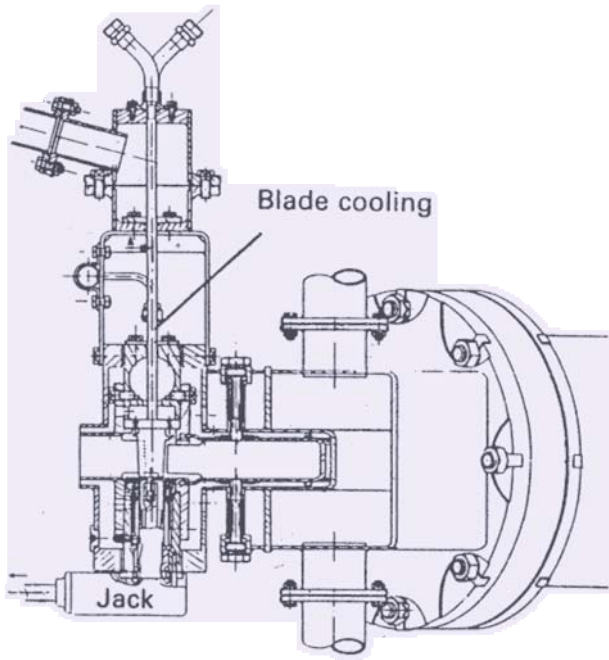
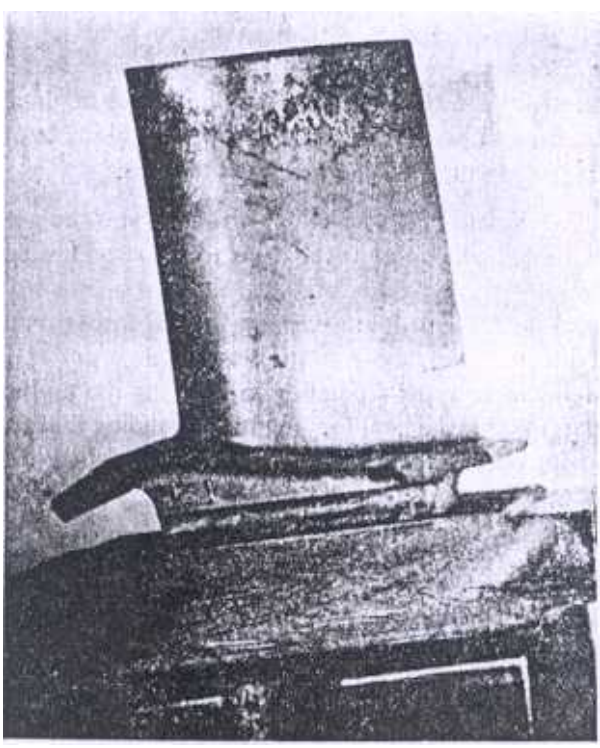


Figure 15.



Figure

at 870°C, comes essentially from the increase in the volume fraction of hardening phase γ' (Ni_3Ti , Al). The improvement in material production processes has made it possible to achieve of 50 per cent. Continuing with this advance poses a number of metallurgical problems that result in a decrease of the ductility in creep. It then becomes necessary to reduce the number of grain boundaries and orient them parallel to the direction of centrifugal and thermal stresses in the blade, in order to improve ductility and creep strength. Fig. 17 shows this evolution between equiaxial IN 100, columnar DS 200 Hf and single-crystal AM1. By accepting to use very sophisticated manufacturing processes (Fig. 18) alloys free from grain boundaries and having a volume fraction of γ' that can go as high as 70 per cent can be produced which offers to improve the creep strength of these materials by 40 to 50°C.

SNECMA, in association with the Imphy S.A. company, the Ecole des Mines de Paris and ONERA, has selected a family of alloys, one of which is the AM1.

The crystallographic direction in which the rate of grain growth is highest is $\langle 001 \rangle$, and it happens that this direction exhibits a relatively low Young's modulus as this example shows for a nickel alloy at 20°C.

$E_{\text{equiaxial}}$	$E_{\langle 001 \rangle}$	$E_{\langle 011 \rangle}$	$E_{\langle 111 \rangle}$
220 GPa	130 GPa	220 GPa	290 GPa

One consequence of this low Young's modulus in the lengthwise direction of the single crystal blades is an almost proportional decrease in the amplitude of the thermal stresses in the structure. From this, we get a spectacular improvement in thermal fatigue strength.

However, these materials do pose many modelling problems, such as the variation of the plastic gap between σ_{failure} and $\sigma_{0.2}$ as a function of the temperature, and the sensitivity to the shape factors at medium temperature. Their anisotropic behaviour also requires three-dimensional finite element models which are today reserved for static and dynamic linear analysis (Fig. 19).

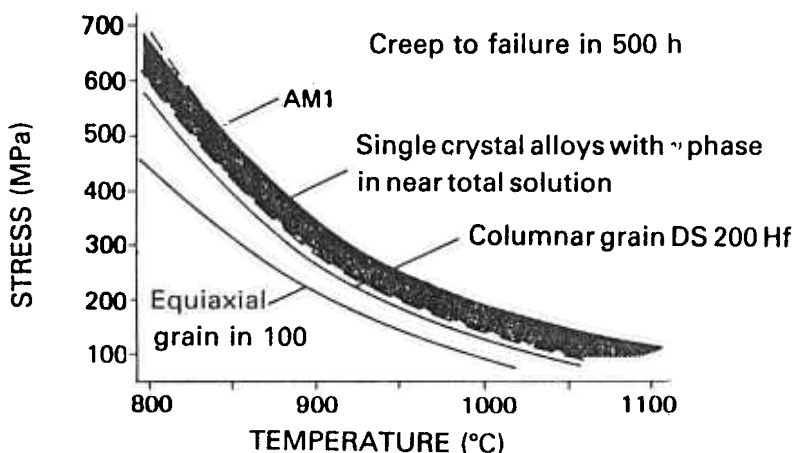


Figure 17.

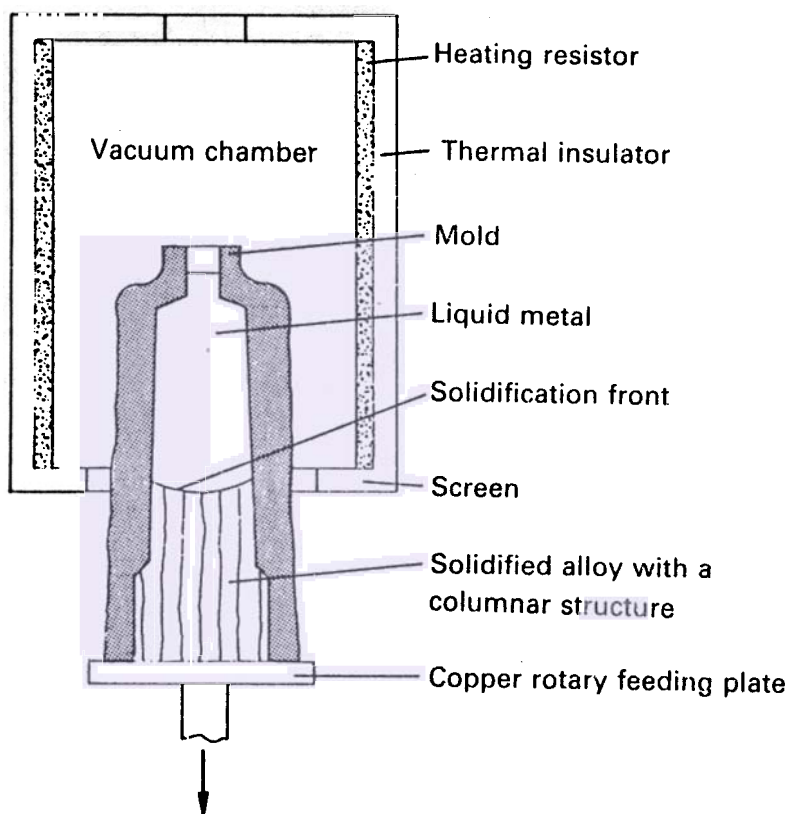


Figure 18.

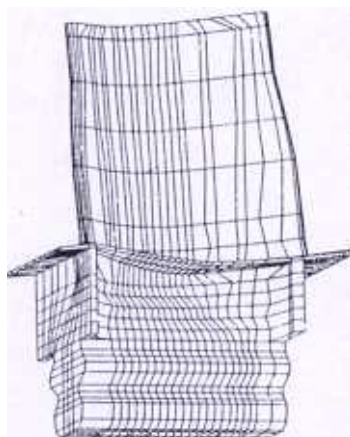


Figure 19. Rotation around $DE \gamma = 110^\circ$, rotation around $DE \chi = -10^\circ$ (M88-15 AUBE IIP blade).

The specific mechanical aspects of single crystal alloys still need to be known in greater depth in order to appropriately adapt the viscoplastic simulation codes, the structural design methods and the properties of the material, but in all probability these alloys will be the foundation for turbine blade developments in the decade to come.

9. CONCLUSION

After struggling against fatigue and creep damage by cooling the structures and improving material characteristics, the only thing left to the engineer is to analyse and model those phenomena. The various methods and tools described in this paper are, one of the best approaches to modelling thermal fatigue and creep phenomena. If a general finite element code of cyclic viscoplasticity and materials characteristics is available, these methods can be extended to any type of component commonly encountered in the industrial environment. Today, SNECMA is extending this approach to all hot, highly stressed components of a turbojet engine.

REFERENCES

1. Herteman, J.P., *L'évolution des matériaux pour aubes de turbine, Matériaux et techniques*, 1985.
2. Gastebois, Ph. & Lagrange, J.P., *Dimensionnement et thermomécanique des aubes de turbines aéronautiques*, Revue générale de thermique n°, 1985, 282-283.
3. Senechal, P., *Introduction des effets de fatigue oligocyclique et de fluage dans la conception d'un turboréacteur de technologie avancée*, Semaine GIFAS au Brésil du 7 au 10 juin 1982.
4. Kaufman, A., Tong, M., Saltsman, J.F. & Halford, G.R., *Structural analysis of turbine blades using unified constitutive models*, Conference Computers in Engine Technology, Cambridge, 1987.
5. Chaboche, J.L., *Stress calculations for lifetime prediction in turbine blades*, Symposium sur la Fatigue à Haute Température, STROSS, 1972.
6. Chaboche, J.L., *Sur les lois de comportement des matériaux sous sollicitations monotones ou cycliques*, La Recherche Aérospatiale n° 1983-5, French and English editions.
7. Chaboche, J.L., *EVPCYCL un code éléments finis en viscoplasticité cyclique*, La Recherche Aérospatiale n° 1986-2, French and English editions.
8. Lemaitre, J. & Chaboche, J.L., *Mécanique des matériaux solides*, Dunod, Paris, 1985.
9. Remy, L., *Méthodologie de la fatigue thermique. Journées internationales de printemps*, Paris, 1986.
10. Golinval, J.C., Mascarrel, J.P. & Geradin, M., *Three Dimensional Turbine Blade Analysis in Thermo-Viscoplasticity - to be published in La Recherche Aérospatiale*.